

# ChemComm

Accepted Manuscript



This article can be cited before page numbers have been issued, to do this please use: D. Wang, B. Wang, Y. Ding, H. Wu and P. WU, *Chem. Commun.*, 2016, DOI: 10.1039/C6CC06779D.



This is an *Accepted Manuscript*, which has been through the Royal Society of Chemistry peer review process and has been accepted for publication.

*Accepted Manuscripts* are published online shortly after acceptance, before technical editing, formatting and proof reading. Using this free service, authors can make their results available to the community, in citable form, before we publish the edited article. We will replace this *Accepted Manuscript* with the edited and formatted *Advance Article* as soon as it is available.

You can find more information about *Accepted Manuscripts* in the [Information for Authors](#).

Please note that technical editing may introduce minor changes to the text and/or graphics, which may alter content. The journal's standard [Terms & Conditions](#) and the [Ethical guidelines](#) still apply. In no event shall the Royal Society of Chemistry be held responsible for any errors or omissions in this *Accepted Manuscript* or any consequences arising from the use of any information it contains.

Journal Name

COMMUNICATION

## A Novel Acid-Base Bifunctional Catalyst of ZSM-5@Mg<sub>3</sub>Si<sub>4</sub>O<sub>9</sub>(OH)<sub>4</sub> with Core/Shell Hierarchical Structures and Superior Activities in Tandem Reactions†

 Received 00th January 20xx,  
Accepted 00th January 20xx

DOI: 10.1039/x0xx00000x

Darui Wang, Bo Wang, Yu Ding, Haihong Wu and Peng Wu\*

www.rsc.org/

**Hierarchically core/shell structured base-acid bifunctional catalyst of ZSM-5@Mg<sub>3</sub>Si<sub>4</sub>O<sub>9</sub>(OH)<sub>4</sub> was successfully prepared through a simple hydrothermal reaction between the silica species on ZSM-5 crystal surface and the Mg<sup>2+</sup> source in basic solution. The obtained catalyst showed superior activity and stability in one-pot deacetalization-Knoevenagel condensation reaction.**

Recently, chemists have paid great attentions to the development of one-pot and/or tandem organic reactions owing to their natures of simple operations and process intensification.<sup>1-3</sup> Among the various systems designed to satisfy this idea, many approaches are taking homogeneous catalysis systems. Despite the high activity and selectivity, homogeneous catalysts are difficult to recycle and reuse, which will inevitably enhance the cost and even cause pollution of the environment and products.<sup>4,5</sup> Furthermore, the one-pot reactions catalyzed by bifunctional acid-base catalysts are hardly developed in the homogeneous phase systems because the acid and base sites are easily deactivated each other. Therefore, the development of heterogeneous catalysts, especially acid-base bifunctional catalysts with immobilized active sites that can effectively promote one-pot reactions have currently received great interests.<sup>6-12</sup>

The combination of acid and base catalysts for the tandem process is recognized as an attractive approach since the acidic and basic functions can activate electrophiles and nucleophiles, respectively.<sup>13-20</sup> To date, acid-base bifunctional catalysts hosted on the solid matrixes, such as silica, polymer and graphene oxide, have been reported.<sup>16</sup> For instance, Angeletti group<sup>17</sup> developed a bifunctional system that the silanols originating from MCM-41 mesosilica acted as acid sites whereas the 1,8-bis(dimethylaminonaphthalene) functional groups immobilized therein served as basic sites useful in acid-

base tandem reactions. In particular, Davis<sup>18</sup> and Shanks groups<sup>19</sup> explored cooperative acid-base catalysts employing an aminopropyl-functionalized SO<sub>3</sub>H-SBA-15 mesosilica. Moreover, the amino group-functionalized metal-organic framework, MIL-101(Al)-NH<sub>2</sub>, has been synthesized using a solvothermal method and employed as a bifunctional acid-base catalyst for tandem deacetalization-Knoevenagel condensation reaction.<sup>20</sup> And the amine-functionalized graphene oxide containing carboxylic acid was also prepared by a facile one-step silylation approach and used as a bifunctional catalyst.<sup>15</sup> Although the fruitful achievements have been obtained in this research field, however, they often suffer from complicated protection-deprotection procedures that are required to avoid neutralization. In addition, the bifunctional catalysts with spatially well defined acid and base sites are needed to develop with the purpose to improve the unsatisfactory catalytic activity in existing systems due to the enhanced steric hindrance.

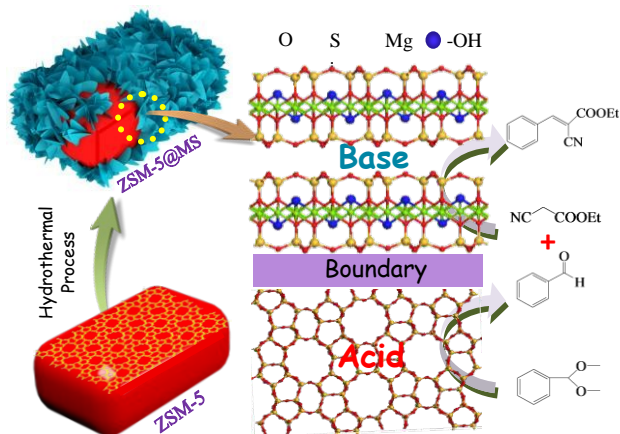
Crystalline aluminosilicate zeolites possess integral channel systems of well-defined microporosity and intrinsic solid acidity.<sup>21</sup> Considering these unique properties, incorporating basic components into acidic zeolites can lead to excellent acid-base bifunctional catalyst. Kubota et al<sup>22</sup> once employed the uncalcined Beta zeolite containing tetraethylammonium (TEA<sup>+</sup>) cations to catalyze the Knoevenagel condensation. The SiO<sup>-</sup> moieties located at the pore mouth and residual TEA<sup>+</sup> cations were presumed to be the active basic sites. Unfortunately, the small sized TEA<sup>+</sup> cations were extracted readily out of the channels of beta zeolites by acid treatment, and suffered leaching problem in liquid-phase organic reactions. On the other hand, supporting solid base alkali-earth metal oxides on zeolites by conventional wetness impregnation (IM) method is a simple preparation technology. Various acid-base bifunctional catalysts, such as CaO/ITQ-2,<sup>23</sup> MgO/MCM-22<sup>23,24</sup> and MgO/ZSM-5,<sup>25</sup> have thus been successfully prepared. However, these catalysts may encounter the drawbacks of basic active sites losing, micropores blocking and unsatisfied catalytic activity because of a relatively weak metal oxides-zeolite interaction.

Shanghai Key Laboratory of Green Chemistry and Chemical Process, School of Chemistry and Molecular Engineering, East China Normal University, North Zhongshan Rd. 3663, Shanghai 200062, China

E-mail: pwwu@chem.ecnu.edu.cn

Fax: (+)86-21-62232292

†Electronic Supplementary Information (ESI) available: Details of experimental procedures and material characterization. See DOI: 10.1039/x0xx00000x



**Scheme 1** Schematic illustration of the preparation procedures for ZSM-5@Mg<sub>3</sub>Si<sub>4</sub>O<sub>9</sub>(OH)<sub>4</sub> and its application to acid-base one-pot reaction.

Herein, we communicate a novel method for preparing hierarchically core/shell structured acid-base bifunctional catalyst. As illustrated in Scheme 1, this process involved the dissolving of silica species off the ZSM-5 crystal surface in base solution and then *in situ* reaction with magnesium cations to form the flower-like magnesium silicate, giving rise to a composite material of ZSM-5@Mg<sub>3</sub>Si<sub>4</sub>O<sub>9</sub>(OH)<sub>4</sub> with ZSM-5 as core and Mg<sub>3</sub>Si<sub>4</sub>O<sub>9</sub>(OH)<sub>4</sub> as shell. The special core/shell structure was similar to that in the previous literatures.<sup>26,27</sup> Hydrothermal reaction between SiO<sub>2</sub> and Mg<sup>2+</sup> took place as follows: 4SiO<sub>2</sub> + 3Mg<sup>2+</sup> + 5H<sub>2</sub>O = Mg<sub>3</sub>Si<sub>4</sub>O<sub>9</sub>(OH)<sub>4</sub> + 6H<sup>+</sup>. The resultant catalysts showed a superior activity and stability in one-pot deacetalization-Knoevenagel condensation reaction with ZSM-5 acting as acid sites and Mg<sub>3</sub>Si<sub>4</sub>O<sub>9</sub>(OH)<sub>4</sub> serving as basic sites. This novel hydrothermal method was featured by the simultaneous construction of a hierarchical structure and spatially well-defined stable basic sites.

Core/shell structured ZSM-5@Mg<sub>3</sub>Si<sub>4</sub>O<sub>9</sub>(OH)<sub>4</sub> materials were prepared readily by hydrothermal reaction at an optimal temperature of 120 °C for 3 h (Fig. S1 and S2, ESI<sup>†</sup>). The coating of hierarchically flower-like Mg<sub>3</sub>Si<sub>4</sub>O<sub>9</sub>(OH)<sub>4</sub> on ZSM-5 crystals by this novel method has been traced with the powder XRD patterns and FT-IR spectra. The XRD pattern of the pristine ZSM-5 was characteristic of a typical MFI structure (Fig. S3a, ESI<sup>†</sup>). After the hydrothermal reaction in Mg<sup>2+</sup> containing solution, the resultant ZSM-5@Mg<sub>3</sub>Si<sub>4</sub>O<sub>9</sub>(OH)<sub>4</sub> showed additional diffractions around 19.5°, 34.5°, 36.2° and 60.5° in high angle region (Fig. S3b, ESI<sup>†</sup>), which are indexed as the [020], [200], [-133] and [-332] planes of magnesium silicate (Mg<sub>3</sub>Si<sub>4</sub>O<sub>9</sub>(OH)<sub>4</sub>, JCPDS No. 03-0174).<sup>28,29</sup> In addition, no peaks related to other crystalline magnesium compounds were observed, indicating that Mg<sub>3</sub>Si<sub>4</sub>O<sub>9</sub>(OH)<sub>4</sub> was the only phase newly developed. FT-IR spectroscopy (Fig. S4, ESI<sup>†</sup>) was utilized to characterize the formed functional groups. Compared with pristine ZSM-5, three new bands emerged at around 557 cm<sup>-1</sup>, 665 cm<sup>-1</sup> and 1050 cm<sup>-1</sup> for ZSM-5@Mg<sub>3</sub>Si<sub>4</sub>O<sub>9</sub>(OH)<sub>4</sub>, which are ascribed to the Si-O-Mg stretching vibrations.<sup>30,31</sup> This further verified the formation of magnesium silicate after hydrothermal reaction. As shown in Fig. S5 (ESI<sup>†</sup>), the synthesized magnesium silicate was characteristic of the talc

structure. Talc is composed of three infinite layers formed by the sharing of oxygen ions at three corners of the silica tetrahedron, a layer of octahedral-coordinated magnesium/hydroxide ions holds two layers of tetrahedral-coordinated silicon/oxygen ions together as a three-layer sheet. And the crystals are held together by Van der Waals forces acting across adjacent tetrahedral layers.<sup>28</sup>

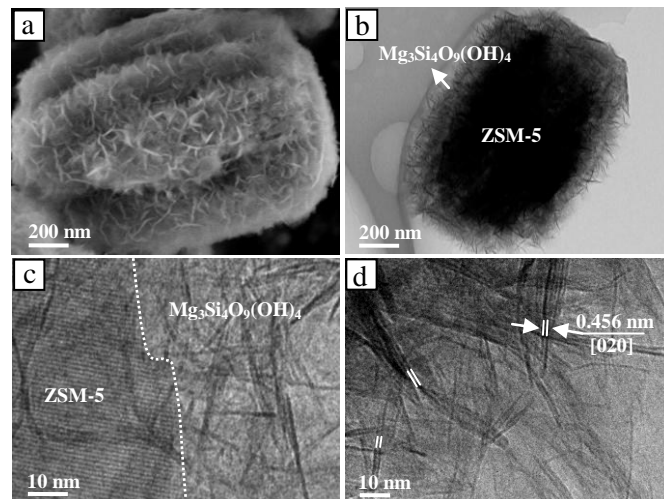


**Fig. 1** SEM image (a) and TEM images (b, c and d) of ZSM-5@Mg<sub>3</sub>Si<sub>4</sub>O<sub>9</sub>(OH)<sub>4</sub>.

The SEM and TEM images showed that the pristine ZSM-5 was of the polycrystalline particles with a relatively smooth surface and a regular size of 1 - 2 μm (Fig. S6, ESI<sup>†</sup>). After the hydrothermal reaction in Mg<sup>2+</sup> containing solution, the as-fabricated ZSM-5@Mg<sub>3</sub>Si<sub>4</sub>O<sub>9</sub>(OH)<sub>4</sub> was evenly covered with a shell made up of flower-like nanosheets, forming a core/shell structured materials resembling the origin shape (Fig. 1a). The structure of thus prepared ZSM-5@Mg<sub>3</sub>Si<sub>4</sub>O<sub>9</sub>(OH)<sub>4</sub> was further investigated by TEM investigation. The shell was composed of flexible nanosheets with the thickness of about 120 nm (Fig. 1b). A representative HRTEM image clearly showed the junction between the shell and core, in which the flower-like nanosheets and the crystalline ZSM-5 crystal grew connectedly (Fig. 1c). As shown in the enlarged image of lamellar nanosheets (Fig. 1d), the distance of the adjacent lattice fringes was determined to be 0.456 nm, corresponding well to the *d*<sub>020</sub> spacing value of Mg<sub>3</sub>Si<sub>4</sub>O<sub>9</sub>(OH)<sub>4</sub> (JCPDS No. 03-0174).<sup>28</sup>

Solid state <sup>29</sup>Si NMR spectroscopy is a powerful tool to study the chemical environment and bonding patterns of the SiO<sub>4</sub> units. The pristine ZSM-5 showed the only peaks at -114 and -106 ppm, corresponding to Q<sup>4</sup> groups (Fig. S7, ESI<sup>†</sup>). This result indicated all Si atoms were interconnected by oxygen bridge. After hydrothermal reaction, the ZSM-5@Mg<sub>3</sub>Si<sub>4</sub>O<sub>9</sub>(OH)<sub>4</sub> showed a broad peak at 96 ppm, corresponding to Q<sup>3</sup> groups, which was consistent with a talc-like crystal structure with SiO<sub>4</sub> structural units forming layers through networking (Fig. 2A).<sup>32,33</sup> The result agreed well with its Mg<sub>3</sub>Si<sub>4</sub>O<sub>9</sub>(OH)<sub>4</sub> composition. Besides, a weak chemical shift at -87 ppm assigned to Q<sup>2</sup> was observed, which was due to the amorphous Si-O species situated on the zeolite surface.

The above results confirmed that magnesium silicate was produced under basic conditions and showed the lamellar

structure. The XPS data also provided the similar information about the structure. As shown in Fig. S8 (ESI<sup>†</sup>), the binding energy of Si 2p was 102.8 eV for ZSM-5@Mg<sub>3</sub>Si<sub>4</sub>O<sub>9</sub>(OH)<sub>4</sub>, 0.6 eV lower than 103.4 eV for pristine ZSM-5. The difference in binding energy for these two kinds of silicon species is in agreement with the literature.<sup>34</sup> In addition, the state of Al was also investigated by <sup>27</sup>Al MAS NMR (Fig. S9, ESI<sup>†</sup>), the microenvironment of Al became more asymmetric in coordination states after incorporating Mg<sub>3</sub>Si<sub>4</sub>O<sub>9</sub>(OH)<sub>4</sub>.

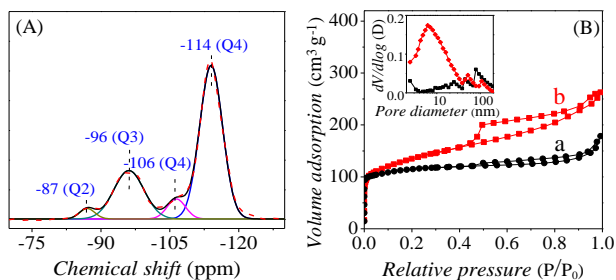


**Fig. 2** Solid state <sup>29</sup>Si NMR spectra of ZSM-5@Mg<sub>3</sub>Si<sub>4</sub>O<sub>9</sub>(OH)<sub>4</sub> (A); N<sub>2</sub> adsorption/desorption isotherm (B) of pristine ZSM-5 (a) and ZSM-5@Mg<sub>3</sub>Si<sub>4</sub>O<sub>9</sub>(OH)<sub>4</sub> (b), insets showed the BJH pore size distribution.

The N<sub>2</sub> adsorption isotherms clearly revealed a significant change in porosity after the hydrothermal reaction. The pristine ZSM-5 showed a typical type I isotherm (Fig. 2Ba), characteristic of microporous materials. That of ZSM-5@Mg<sub>3</sub>Si<sub>4</sub>O<sub>9</sub>(OH)<sub>4</sub> was characteristic of both type I and type IV (Fig. 2Bb), implying the presence of multiple pore systems. The slowly increased uptake in the P/P<sub>0</sub> region of 0.2 - 0.9 was probably because of relatively irregular mesopores ascribed to the disordered assembly of the flexible Mg<sub>3</sub>Si<sub>4</sub>O<sub>9</sub>(OH)<sub>4</sub> nanosheets. The pore size distribution showed that ZSM-5@Mg<sub>3</sub>Si<sub>4</sub>O<sub>9</sub>(OH)<sub>4</sub> possessed the mesopores with 2 - 20 nm diameters, which were absent in the pristine ZSM-5 sample. As shown in Table S1 (ESI<sup>†</sup>), the mesopore surface areas increased from 31 m<sup>2</sup> g<sup>-1</sup> to 193 m<sup>2</sup> g<sup>-1</sup> and mesopore volumes increased from 0.10 cm<sup>3</sup> g<sup>-1</sup> to 0.26 cm<sup>3</sup> g<sup>-1</sup> when the Mg content was 10.0 wt%. These novel materials, with confined space and enhanced mass transfer rate, would have potential applications as hierarchical catalysts.

The acidity and basicity were investigated by NH<sub>3</sub>-TPD and CO<sub>2</sub>-TPD techniques, respectively. Compared with the pristine ZSM-5 (Fig. S11a, ESI<sup>†</sup>), ZSM-5@Mg<sub>3</sub>Si<sub>4</sub>O<sub>9</sub>(OH)<sub>4</sub> (Fig. S11b, ESI<sup>†</sup>) possessed slightly lower total acid quantity of 0.38 mmol g<sup>-1</sup>. And the strong acid quantity decreased from 0.143 mmol g<sup>-1</sup> to 0.063 mmol g<sup>-1</sup> while middle strong acid quantity increased from 0.118 mmol g<sup>-1</sup> to 0.268 mmol g<sup>-1</sup>, which may be due to the sacrificing of ZSM-5 crystal or a partial cation exchange between Mg<sup>2+</sup> and H<sup>+</sup> during hydrothermal reaction. On the contrary, the total basic quantity was 0.24 mmol g<sup>-1</sup> for ZSM-5@Mg<sub>3</sub>Si<sub>4</sub>O<sub>9</sub>(OH)<sub>4</sub> (Fig. S12b, ESI<sup>†</sup>), much higher than 0.14 mmol g<sup>-1</sup> of pristine ZSM-5 (Fig. S12a, ESI<sup>†</sup>). Thus, the newly formed magnesium silicate was speculated to be potential basic active sites, and hierarchical ZSM-5@Mg<sub>3</sub>Si<sub>4</sub>O<sub>9</sub>(OH)<sub>4</sub> could act as acid-base bifunctional catalyst in one-pot reaction.

To demonstrate the synthetic controllability, the products were synthesized with different Mg contents, corresponding to

theoretical loading amounts of 5.0, 7.5, 10.0, 12.5 and 15.0 wt%. ICP analysis indicated the Mg contents actually loaded on zeolite were 5.1, 7.6, 10.0, 12.6 and 15.1 wt%, respectively. Thus, this method gave a utilization efficiency of Mg<sup>2+</sup> source close to 100 % and easily controlled the Mg loading amounts in a relatively wide range. Fig. S13 (ESI<sup>†</sup>) showed the SEM images of ZSM-5@Mg<sub>3</sub>Si<sub>4</sub>O<sub>9</sub>(OH)<sub>4</sub> with different Mg contents. At lower Mg loadings of 5.1 wt%, the rough surfaces were already observed clearly. Certainly, larger amount nanosheets were formed when the Mg contents reached 15.1 wt%. In XRD patterns (Fig. S14, ESI<sup>†</sup>), the intensity of peaks indexed as Mg<sub>3</sub>Si<sub>4</sub>O<sub>9</sub>(OH)<sub>4</sub> were enhanced with increasing Mg contents.

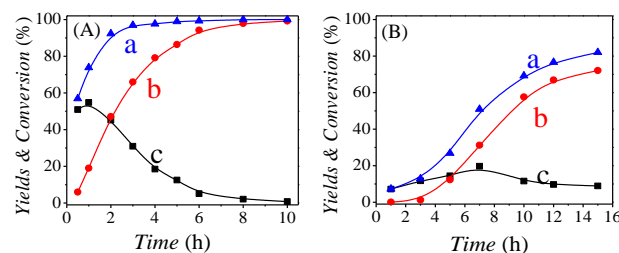


**Fig. 3** The kinetics of one-pot deacetalization-Knoevenagel condensation reaction over ZSM-5@Mg<sub>3</sub>Si<sub>4</sub>O<sub>9</sub>(OH)<sub>4</sub> (A) and MgO/ZSM-5 (B): conversion of benzaldehyde dimethylacetal (a), yields of benzylidene ethyl cyanoacetane (b) and benzaldehyde (c). Reaction conditions: catalyst, 50 mg; benzaldehyde dimethylacetal, 5 mmol; ethyl cyanoacetate, 7.5 mmol; H<sub>2</sub>O, 5 mmol; toluene, 2 mL.

The potential use of ZSM-5@Mg<sub>3</sub>Si<sub>4</sub>O<sub>9</sub>(OH)<sub>4</sub> as a bifunctional acid-base catalyst for one-pot reactions was investigated next. ZSM-5@Mg<sub>3</sub>Si<sub>4</sub>O<sub>9</sub>(OH)<sub>4</sub> was employed to promote the formation of benzylidene ethylcyanoacetane (BE) from the reaction between benzaldehyde dimethylacetal (BD) and ethyl cyanoacetate, which takes place through sequential deacetalization and Knoevenagel condensation processes (Fig. S15, ESI<sup>†</sup>).<sup>35</sup> Inspecting the time course of the process (Fig. 3A), it is obvious that BE was efficiently generated from BD via a pathway involving initial formation of benzaldehyde intermediate, and the yield of BE reached 94.2% at 6 h. For comparison, the pristine ZSM-5 and conventional acid-base catalyst of MgO/ZSM-5 prepared by wetness impregnation method were also applied for this one pot reaction. When the pristine ZSM-5 was used as the catalyst (Fig. S16, ESI<sup>†</sup>), the second step, involving Knoevenagel condensation of benzaldehyde with ethyl cyanoacetate, did not take place efficiently. As a result, only benzaldehyde was produced because pristine ZSM-5 only served as an acid catalyst for the deacetalization step. Also, the one-pot reaction took place when conventional MgO/ZSM-5 was utilized (Fig. 3B), but the reaction rate was much lower than that of the ZSM-5@Mg<sub>3</sub>Si<sub>4</sub>O<sub>9</sub>(OH)<sub>4</sub> catalyst, giving only 22.1% yield of BE at 6 h. In comparison to ZSM-5@Mg<sub>3</sub>Si<sub>4</sub>O<sub>9</sub>(OH)<sub>4</sub>, MgO/ZSM-5 showed significantly decrease in the micro/mesopore surface area and micro/mesopore volume due to the pores blocking (Fig. S10 and Table S1, ESI<sup>†</sup>). In addition, MgO/ZSM-5 (Fig. S11c and 12c, ESI<sup>†</sup>) possessed less acid/base active sites than ZSM-5@Mg<sub>3</sub>Si<sub>4</sub>O<sub>9</sub>(OH)<sub>4</sub>. These observations clearly demonstrated that ZSM-5@Mg<sub>3</sub>Si<sub>4</sub>O<sub>9</sub>(OH)<sub>4</sub> possessed both hierarchical pores and plentiful acid/base active sites that served as an

effective catalyst for respective deacetalization and Knoevenagel condensation reactions.

In addition, when the condensation reactant ethyl cyanoacetate was substituted by malononitrile, the final product yield increased obviously on ZSM-5@Mg<sub>3</sub>Si<sub>4</sub>O<sub>9</sub>(OH)<sub>4</sub>. The BE conversion reached 100% and the yield of benzylidene malononitrile (BM) was 99.7% after 90 min (Fig. S17b, ESI<sup>†</sup>), and also showed faster reaction rate than MgO/ZSM-5 (Fig. S17c, ESI<sup>†</sup>) due to its special hierarchical structure and more active sites. In a following step, the stabilities of ZSM-5@Mg<sub>3</sub>Si<sub>4</sub>O<sub>9</sub>(OH)<sub>4</sub> and MgO/ZSM-5 were checked by recycling the catalyst (Fig. S18, ESI<sup>†</sup>). No notable changes in activity were observed over eight cycles for ZSM-5@Mg<sub>3</sub>Si<sub>4</sub>O<sub>9</sub>(OH)<sub>4</sub>. However, MgO/ZSM-5 lost about 18.3% of its initial activity and the BE yield decreased from 91.8% to 60.5% after eight reaction runs. The activity loss was presumed to be mainly due to loss of basic active sites and coke formation. For the reused ZSM-5@Mg<sub>3</sub>Si<sub>4</sub>O<sub>9</sub>(OH)<sub>4</sub> catalyst, the framework structure was maintained well (Fig. S19, ESI<sup>†</sup>), and the Mg content loss was prevented, according to ICP analysis, we can calculate that Mg contents were 9.8 wt% and 4.3 wt% for ZSM-5@Mg<sub>3</sub>Si<sub>4</sub>O<sub>9</sub>(OH)<sub>4</sub> and MgO/ZSM-5 after eight recycling runs, respectively. Moreover, the coke formation was also effectively prevented for ZSM-5@Mg<sub>3</sub>Si<sub>4</sub>O<sub>9</sub>(OH)<sub>4</sub> due to the hierarchical structure, only 4.1 wt% coke was observed by TG analysis, but coke content reached up to 7.4 wt% for conventional MgO/ZSM-5. This result was caused by the shorter diffusion path length in the hierarchical catalyst. The stability was further checked by treating ZSM-5@Mg<sub>3</sub>Si<sub>4</sub>O<sub>9</sub>(OH)<sub>4</sub> at 700 °C for 24 h in a flow of air, no noticeable change was observed according to XRD analysis (Fig. S20, ESI<sup>†</sup>).

Importantly, the synthetic strategy is quite general. We have successfully prepared other acid-base bifunctional catalysts by varying the types of zeolites in the hydrothermal reaction, such as mordenite@Mg<sub>3</sub>Si<sub>4</sub>O<sub>9</sub>(OH)<sub>4</sub>, Beta@Mg<sub>3</sub>Si<sub>4</sub>O<sub>9</sub>(OH)<sub>4</sub> and MCM-22@Mg<sub>3</sub>Si<sub>4</sub>O<sub>9</sub>(OH)<sub>4</sub> (Fig. S21, ESI<sup>†</sup>).

In summary, we have developed a facile route for preparing hierarchically core/shell structured base-acid bifunctional catalyst, ZSM-5@Mg<sub>3</sub>Si<sub>4</sub>O<sub>9</sub>(OH)<sub>4</sub> was successfully prepared through a simple hydrothermal reaction in base solution. The flower-like Mg<sub>3</sub>Si<sub>4</sub>O<sub>9</sub>(OH)<sub>4</sub> nanosheets can readily grow on the surface of zeolite to form a hierarchically core/shell structure without any pretreatment or binding agent. Furthermore, the obtained ZSM-5@Mg<sub>3</sub>Si<sub>4</sub>O<sub>9</sub>(OH)<sub>4</sub> catalyst showed super activity and stability in tandem deacetalization-Knoevenagel condensation reaction. In particular, we found that this simple method was also applicable to other zeolites (e.g. mordenite, Beta and MCM-22) with different framework topologies.

The authors gratefully acknowledge the financial supports from NSFC of China (21533002, 21373089, 21373088), and China Ministry of Science and Technology under contract of 2016YFA0202804.

## Notes and references

- J. M. Lee, Y. Na, H. Han and S. Chang, *Chem. Soc. Rev.*, 2004, **33**, 302.
- J.-C. Wasilke, S. J. Obrey, R. T. Baker and G. C. Bazan, *Chem. Rev.*, 2005, **105**, 1001. DOI: 10.1039/C6CC06779D
- M. J. Climent, A. Corma and S. Iborra, *Chem. Rev.*, 2011, **111**, 1072.
- C. Gunanathan, Y. Ben-David and D. Milstein, *Science*, 2007, **317**, 790.
- T. Zweifel, J.-V. Naubron and H. Grützmacher, *Angew. Chem. Int. Ed.*, 2009, **48**, 559.
- F. Gelman, J. Blum and D. Avnir, *J. Am. Chem. Soc.*, 2002, **124**, 14460.
- A. Corma, T. Ródenas and M. J. Sabater, *J. Catal.*, 2011, **279**, 319.
- N. R. Shiju, A. H. Alberts, S. Khalid, D. R. Brown and G. Rothenberg, *Angew. Chem. Int. Ed.*, 2011, **50**, 9615.
- K. Motokura, M. Tada and Y. Iwasawa, *J. Am. Chem. Soc.*, 2009, **131**, 7944.
- Y. Huang, S. Xu and V. S.-Y. Lin, *Angew. Chem., Int. Ed.*, 2011, **50**, 661.
- M. Sasidharan, S. Fujita, M. Ohashi, Y. Goto, K. Nakashima and S. Inagaki, *Chem. Commun.*, 2011, **47**, 10422.
- S. J. Broadwater, S. L. Roth, K. E. Price, K. Muris, M. Kobašljica and D. T. McQuade, *Org. Biomol. Chem.*, 2005, **3**, 2899.
- K. Motokura, M. Tada and Y. Iwasawa, *J. Am. Chem. Soc.*, 2009, **131**, 7944.
- V. Rodionov, H. F. Gao, S. Scroggins, D. A. Unruh, A. J. Avestro and J. M. J. Fréchet, *J. Am. Chem. Soc.*, 2010, **132**, 2570.
- F. Zhang, H. Jiang, X. Li, X. Wu, and H. Li, *ACS Catal.*, 2014, **4**, 394.
- E. L. Margelefsky, R. K. Zeidan and M. E. Davis, *Chem. Soc. Rev.*, 2008, **37**, 1118.
- E. Angeletti, C. Canepa, G. Martinetti and P. Venturello, *J. Chem. Soc., Perkin Trans.* 1989, **1**, 105.
- R. K. Zeidan, S. J. Hwang and M. E. Davis, *Angew. Chem. Int. Ed.*, 2006, **45**, 6332.
- S. L. Hruby and B. H. Shanks, *J. Catal.*, 2009, **263**, 181.
- T. Toyao, M. Fujiwaki, Y. Horiuchi and M. Matsuoka, *RSC Adv.*, 2013, **3**, 21582.
- A. Corma, *Chem. Rev.*, 1995, **95**, 559.
- Y. Kubota, Y. Nishizaki, H. Ikeya, M. Saeki, T. Hida, S. Kawazu, M. Yoshida, H. Fujii and Y. Sugi, *Micro. Meso. Mater.*, 2004, **70**, 135.
- J. Liang, X. Hu, J. Wang, X. Ren, X. Yang and J. Zhu, *Catal. Commun.*, 2015, **69**, 174.
- W. Zhang, J. Liang, Y. Liu, S. Sun, X. Ren and M. Jiang, *Chin. J. Catal.*, 2013, **34**, 559.
- S. K. Bej, C. A. Bennett and L. T. Thompson, *Appl. Catal. A, Gen.*, 2003, **250**, 197.
- Y. Bouizi, I. Diaz, L. Rouleau and V. P. Valtchev, *Adv. Func. Mater.*, 2005, **15**, 1955.
- Y. Bouizi, L. Rouleau and V. P. Valtchev, *Chem. Mater.*, 2006, **18**, 4959.
- Y. Wang, G. Wang, H. Wang, C. Liang, W. Cai and L. Zhang, *Chem. -Eur. J.* 2010, **16**, 3497.
- J. Qu, W. Li, C. Y. Cao, X. J. Yin, L. Zhao, J. Bai, Z. Qin and W. G. Song, *J. Mater. Chem.*, 2012, **22**, 17222.
- Z. Zhan and H. C. Zeng, *J. Non-Cryst. Solids*, 1999, **243**, 26.
- J. M. Stencel, E. B. Bradley and F. R. Brown, *Appl. Spectrosc.*, 1980, **34**, 319.
- K. A. Carrado, L. Xu, D. M. Gregory, K. Song, S. Seifert and R. E. Botto, *Chem. Mater.*, 2000, **12**, 3052.
- E. Lippmaa, M. Maegi, A. Samoson, G. Engelhardt and A. -R. Grimmer, *J. Am. Chem. Soc.*, 1980, **102**, 4889.
- R. Guillet-Nicolas, J. -L. Bridot, Y. Seo, M. -A. Fortin and F. Kleitz, *Adv. Funct. Mater.*, 2011, **21**, 4653.
- K. Motokura, M. Tada and Y. Iwasawa, *J. Am. Chem. Soc.* 2009, **131**, 7944.